Jetting Technology: A Way of the Future in Dispensing

Horatio Quinones / Alec Babiarz / Lian Fang

Abstract

Selective dispensing of fluid onto electronic packages without physical contact in a reliable and consistent manner seems a natural alternative to traditional mass transfer methods that are often invasive and lack consistency. For instance, Optoelectronics packages will require small dispensing amounts of numerous materials with a wide range of physical properties; innovative processes must meet this challenge. This paper addresses some proposed solutions including material jetting. With the advances and improvements in technology of the micro-electronic industry and the nano-electronic, the scale of components used has consistently grown smaller. This has allowed for more efficient use of resources (a silicon chip that once held hundreds of transistors now holds millions) and more convenient and consumer friendly products (palm sized computers compared to warehouse sized computers forty years ago). However, as advances lead to decreases in the scale of components, similar advances must be made in the production process in order to assemble these components. One method used in current printed circuit board assembly is attaching components to the board with a surface mount adhesive (SMA). A small dot of adhesive is placed between two pads. Passive components i.e., 0402 can be attached to the board by jetting small dots of SMA material. The component is then placed on top of the SMA. The SMA is then cured, fixing the component in place. When applying the SMA, it is vital that the adhesives not cover any part of the leads, as this may decrease the quality of the solder connection. As components decrease in size, so does the gap between the leads. It is therefore necessary for the size of the adhesive dot to decrease to the same degree as the components decrease. Current technology can produce dots of surface mount adhesive of approximately 20 mil diameter and roughly 0.03-0.04 ml volume. Anticipating the continuing trend in component scale reduction, however, predicts that dots in the 8-10 mil diameter range will be required. The experiment described in this paper attempted to reach this measure of dot size using SMA and silver epoxy materials. Small dot jetting has additional leading edge applications. The present work shows the capability of jetting material in volumes of about 3 nano-liters. The underfilling 3D-packages with small gaps that are required to accomplish thin packages, as well as the underfilling of small die present yet another challenge to the consistency and accuracy of dispensing processes. This paper addresses the underfilling of 3D stacked die by jetting material on die surfaces with small dot to accomplish gaps of just a few microns gap. The challenge of jetting abrasive materials is addressed here by monitoring wearout evolution on the jet itself and corresponding effects on the jetted fluid characteristics. Analytical work on the fluid dynamics is presented and its predictability is demonstrated by experimental data.

Key words: ball-needle, jetting, non-contact, small dots, stagnation zone, underfill

Introduction

Selective dispensing of fluid onto electronic packages without physical contact in a reliable and consistent manner seems a natural alternative to traditional mass transfer methods that are often invasive and lack consistency

This jet works according to the following mechanism. Beginning with an electrical signal, a solenoid is triggered, allowing air pressure into a chamber. This air pressure applies force to a piston-seal, which is attached to a ball-needle, not only lifting the ball-needle, but also compressing a spring on the other side of the piston-seal. As the ball-needle is lifted from its seat, fluid is allowed to flow down and around the ball-needle tip. At the end of the

electrical impulse, the solenoid discharges, releasing the air pressure allowing the force form the compressed spring to slam the ball-needle tip back down into its seat, separating and ejecting a dot from the fluid. There are several parameters that can be adjusted in order to alter the size of the dots produced. The parameter adjustments affect the dots in two different ways, either by changing properties of the fluid, or by changing mechanical properties of the jet. The pressure on the fluid in the syringe was adjusted from 10 to 30 psi. This variation affected how much force pushed the fluid down and around the ball-needle tip when it was raised. The other parameter that affected fluid properties was the nozzle heater temperature setting.

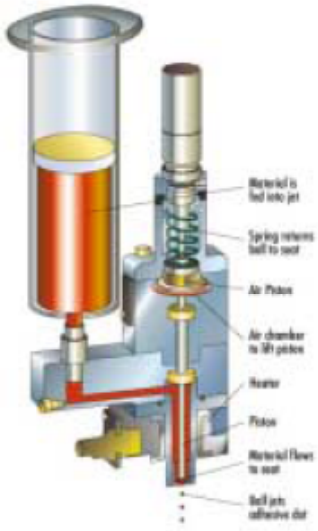

Figure 1. Diagram of the cross section of a jet dispenser

Throughout this paper when reference to temperature is given, the temperature is of the heater setting and not the exact temperature of the fluid. The fluid temperature is always a few degrees less, due to thermal conduction losses in the system. The temperature settings were varied between 30 ^{0}C and 60 ^{0}C. At higher temperature viscosity is decreased which enhances fluid flow reduces surface tension consequently making it easier to separate a dot from the nozzle. Adjusting three different variables can alter the performance of the Jet. The force of the ball-needle is generated by the compression of the spring. By partially compression the spring (pre-load) before the ball-needle is lifted, the force induced by the spring can be increased. The pre-load is applied by screwing the top of the Jet in along a set of threads, and the compression of the spring is then measured as the number of turns. During testing this value was varied form two to four turns of preload. The other parameter regulating the motion of the ball-needle is the stroke length. This is adjusted by turning a micrometer at the top of the Jet; it varies the position of the hard stop of the ball-needle (the distance it is raised off the seat with each stroke). The stroke was tested at values ranging from 0.12 mm up to 1.5 mm. The final parameter tested was the valve on-time. The on-time regulates the time between signals (from when the solenoid was first triggered, raising the ball-needle, to when it was discharged, and the ball-needle began to fall). The valve on-times used in this experiment were 5, 6 and 7 milliseconds. In addition to these parameters, there were several basic alterations made to the actual jet used. While a standard jet uses either a 30 or 60-mil seat, in this experiment 15 and 20 mil seats were used. The nozzle sizes used on the jet were the standard five-mil nozzle and a four-mil nozzle. In addition to using nozzles and seats that were a new size, the micrometer was modified to allow lower pre-load settings. The modification expanded the range of parameters settings for testing

Theory

Numerical analysis was performed to simulate the jetting process and drop formation. Incompressible fluid and non-slip theory were assumed in the simulations presented in this paper. It was determine that the Reynolds number was very low and therefore turbulence conditions were not present. The ball-needle was accelerated by the spring and the transfer of momentum into the fluid causes the drop to form when surface tensions are overcome. The set of equations needed to define the problem consisted of the mass conservation equation [2].

$$\frac{\partial \rho}{\partial t} + \frac{\partial}{\partial x_k}\left[\rho \cdot u_k\right] = 0$$

Where ρ is the fluid density and u_k is the velocity component in the k-coordinate. The momentum conservation equation can be written as

$$\left[\frac{\partial u_i}{\partial t} + u_k \cdot \frac{\partial u_i}{\partial x_k}\right] = \rho \cdot f_i + \frac{\partial \Gamma_{ij}}{\partial x_j}$$

Where f_i is the body force per unit volume along the i-coordinate and Γ_{ij} is the stress tensor.
And the third expression is the constitutive equation relating the shear stresses to the tensions

$$\tau_{ij} = \lambda \frac{\partial u_k}{\partial x_k}\delta_{ij} + \mu\left[\frac{\partial u_i}{\partial x_j} + \frac{\partial u_j}{\partial x_i}\right]$$

Where λ is a second viscosity coefficient, and μ is the dynamic fluid viscosity. The solution of above set of equations is carried out by a method of weighted residuals from variational principles, for instance the mass conservation integral weighted residual for an incompressible fluid equation can be written as. Fluid velocities, Vorticity, stream functions, shear stresses and fluid pressures were computed for various ball-needle velocities and ball-needle location.

$$\left[\int_\Omega d\Omega \cdot \varphi \cdot \frac{\partial \Phi^T}{\partial x_k}\right] \cdot \tilde{u}_k = 0$$

Where $\tilde{u}_k$ is velocity vector approximation to be minimized to satisfy the boundary conditions exactly (weighted residual factor), and Φ^T is the transpose of a "floating function."[3] Figure 2 depicts the diagram of the Jet with the initial boundary conditions.
Figure 3 depicts velocity contour bands resulting from the ball-needle motion prior to impact of the ball-needle and seat. Calculations show that the fluid velocity at the orifice of the nozzle is more than an order of magnitude higher than that of the ball-needle itself. A close-up view, see figure 4, at the ball-needle-seat area shows the resultant velocity field upon impact. By this time fluid flow momentum overcomes the surface tension of the meniscus at the orifice, i.e., the Weber number ($W_e=\rho V_0^2 L/\sigma$) which is the ratio of the inertia force to the capillary force and hence, it can be used as a figure of merit to determine formation of droplets from nozzles

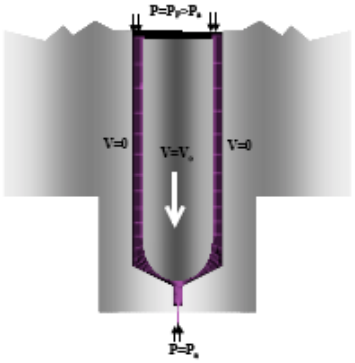

Figure 2. Diagram showing Dirichlet and Neuman boundary conditions.

When a threshold is attained and the drop is formed and jetted at velocities much larger than ball-needle velocity. Recall that the pressure at the smaller diameter of the ball-needle is much larger than that of the seat thereby, inducing high fluid flow at the orifice of the nozzle.

Figure 3. Resultant velocities from numerical calculations.

It should be pointed out that the seat appears to show a large area of slow fluid motion "stagnation zone," near the hardware walls in this particular design. Pressures at the fluid near the contact ball-needle-seat point of contact are very high

indicating that some fluid compressibility should be assumed.

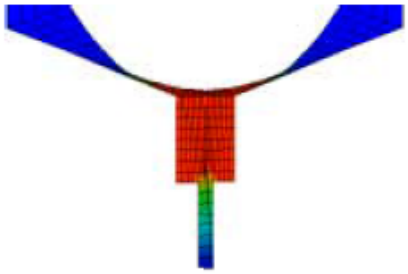

Figure 4. Velocity field upon impact of the ball-needle and the seat.

Figure 5 depicts the pressure band maps upon impact of the ball-needle and the seat computed numerically as explained above.

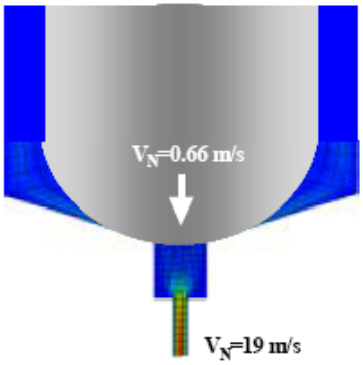

Figure 5. Fluid pressure bands results from numerical analysis upon ball-needle-seat impact.

Experiment

Perhaps the most important parameter used when evaluating the dots (in addition to the quality, or overall shape and roundness), is the measure of the dots size. This was accomplished by looking at not only the diameter of the dots, but also by determining the mass and volume of the dots. These measurements were determined using a variety of methods and calculations. The measure of the dot diameter was often the easiest measurement to acquire, and was often used as a preliminary estimate of the size and quality of the dots. Three methods were used to find the diameter. The first, and most commonly used was the measuring microscope. This machine is simply a Panasonic GP-KR222 camera attached to a Nikon microscope, which is fed into a monitor and a Mycrona Primus measuring system. The dots are focus, then maneuvered using the adjustable stage so that the left and bottom edges of the dot are lined up with crosshairs on the monitor. The x and y measurements on the Mycrona Primus were then zeroed, then the dot moved until the right and top edges were lined up. The resulting x and y displacements of the stage are accurate measurements of the diameter of the dot in the corresponding directions. The one drawback to this method is that it requires human estimation to line up and measure the dot size, so there could be some variation between measurements. Another important consideration was the determination of the edges of the dots. Often (depending on the surface) there was a halo around the edge of the dot. This halo had a negligible height, and was therefore not included in the diameter measurements. The second method of determining the diameter of the dots was the Parmi spi 2500 profiling machine. By reflecting a laser across the surface of the dot, a height profile is generated. This cannot only be used to find the height of the dots, but also, by measuring the extents of the profile, the diameter of the dots can by found. However, the machine could only scan certain surfaces, if the surface was too reflective, the laser could not be focused properly.

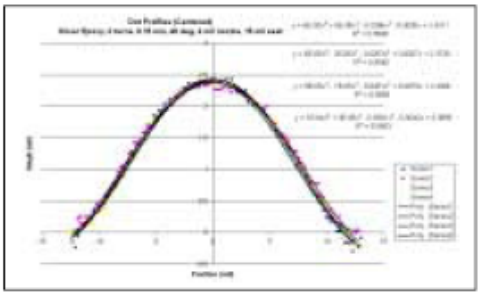

Figure 6. Polynomial fit to the dot profile to calculate the volume/mass of the dots.

The final method for finding the diameter of the dots was to dispense dots in a set pattern on a polished plate. A camera was programmed to photograph each dot ten times, in series, and these photographs were fed into a computer and analyzed by a program called Sherlock. The pictures were examined for shape, size, and

consistency, and the results compiled. Once the diameter of the dot had been determined, and good dots had been obtained, the volume of the dots was the estimated. This was accomplished four ways, two approximations using the measured height Parmi spi 2500 and diameter (from any method), on approximation used the profile, and the last flattened the dots into cylinders and then estimated their volume. The first two methods assumed a certain profile of the dot shape. One used hemispherical profile (assuming the surface of the dot resembled that of a slice of a sphere) and the other used a profile resembled that of and ellipse. Parmi spi 2500 was used to determine the height of the dots; the entire profile measurements were exported to a file. Plotting this data, and fitting a polynomial curve determined the volume. In this experiment, the dots were zeroed (peak occurs at zero on the x axis), and then fit to a fourth degree polynomial (plots are shown in figure 6). This function was then revolved around the y-axis and integrated from zero to its limit, the radius. Figure 7 shows the evolution of this non-contact technology by comparison among different SMA dot sizes jetted onto a metal plate.

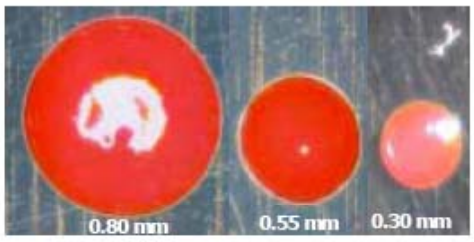

Figure 7. Different SMA dot sizes jetted onto a metal finishing plate

Jetting Underfill Results

The first fluid tested was Namics XS8436-79 underfill fluid. This fluid was tested within the following parameters ranges. The preload was varied between 3 and 4 turns and the temperature was set between 50 and 60^{0}C. Lower temperature values were also investigated (40 and 45^{0}C), but no material could be jetted consistently and with good quality below 50^{0}C. The stroke length was adjusted between 0.2 and 2 mm and the fluid pressure was varied between 13 and 30 psi. A 5-mil nozzle was used with a 15 and 20 mils seat, along with a valve on time of 5 and 7 milliseconds. The best results (as far as achieving the smallest dot possible) were obtained with 4 turns preload, 0.7 mm stroke length, 28-psi fluid pressure and 7 milliseconds on time at 60^{0}C with a 5-mil nozzle and a 15 mils seat. With above settings dots were made that were approximately 17 mils in diameter (0.4318 mm). Using the Cyber-Scan the height was measured to be 1.775 mil. However, this value is believed to be inaccurate. The under-fill fluid is almost transparent, especially when spread as thin as these dots were. Because the Cyber-scan reflects a laser off the surface of the dots, transparency in the fluid could affect how the laser is reflected, affecting the height reading. Based on this height measurement, the volume was calculated (using a hemispherical approximation) to be approximately 3.3E-9 liters. By massing dots dispensed on a glass slide, it was found that each dot weighed (on average) 0.0107 mg. Based on this value, and by adjusting for the density of the fluid (1.2mg/ml), the volume was estimated to be 8.9E-9 liters, suggesting our height calculation was inaccurate. Figure 8 shows a picture of a jetted dot of this underfill material.

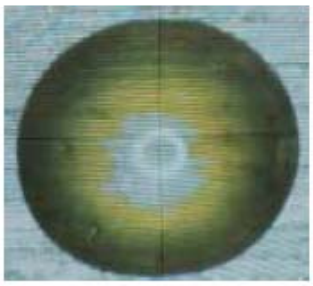

Figure 8. Underfill Material jetted onto a metal finishing surface.

It was discovered that the syringe containing the material needed to be centrifuged to remove bubbles prior to jetting.

Jetting Silver Paste Results

The second material that was used to jet dots was a silver paste solution (used as in the same manner as silver epoxy), formulated by Superior Micro Powders. Dots were made with an average diameter of 18 mils (0.4572 mm) and were found to have a height of 2.4 mils. Using a polynomial approximation the volume was calculated to be 0.007 ml while a hemispherical approximation

estimated the volume as 0.0094 ml. By massing a number of dots on a slide, the average weight per dot was found to be 0.056 mg/dot. While this value is higher than the masses of the other two materials jetted, it is a result of the greater density of the fluid, not of a larger dot volume. While the volume of the dots ejected was small, the diameter was still rather large, relative to the diameter of the dots dispensed with Loctite SMA-3621. The SMA material has a greater viscosity than the Silver paste, and while the volumes of the dots are similar, the diameter of the SMA dots was much smaller (owing to their greater height). With a silver paste with greater viscosity (closer to that of SMA), perhaps dots could be jetted of comparable volume but due to the greater viscosity, with a larger height and a resulting smaller diameter.

Jetting SMA Results

The third fluid tested with the DJ-2000 Jet was Loctite SMA-3621.

Figure 9. SMA dot jetted onto an organic substrate.

This material was the one most tested, and the one jetted at the largest range of settings. During the experiment, the preload was varied from 2 to 4 turns and at stroke lengths between 0.12 and 0.75 mm. The valve was left on from 5-7E-2 seconds and both 4 and 5 mil nozzles were used with 15 and 20 mil seats.

The fluid was pressurized to 10-30 psi and was heated to 40-60 degrees Celsius. The smallest dots were obtained with 2.5 turns of preload at 60 degrees C with a 0.12 mm stroke length. The valve was on for 5E-2 seconds and the fluid was at 23 psi, with a 5-mil nozzle and a 15-mil seat. These dots were 12.5 mil in diameter (0.3175 mm) and a height of about 7.5 mils. Their volume was approximated three different ways. Using a cylindrical approximation the volume was calculated to be 9.25E-6 liters, with a hemispherical approximation the volume was estimated to be 11.45E-6 liters, and an elliptical approximation gave the volume as 10.36E-6 liters. Assuming the mass of this fluid to be 1.2 mg/ml, and taking the average volume approximation, the average weight per dot was estimated to be 0.0124 mg. Figure 10 depicts a picture of SAM jetted directly on an FR4 board. In addition to the experimental results from these tests, there exist data for jet dispensing of Loctite SMA-3621.

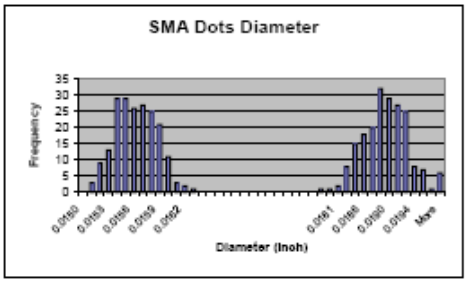

. Figure 10. Histograms showing two distinct distributions for a different parameters setting of a single jet.

It was demonstrated that different parameters setting for the jet would result in two very distinct geometries both, dot diameter and dot volume with no overlap as depicted in figure 10 by the plot of histograms of both settings. The fact that parameter settings can result in a very different dot characteristic makes this non-contact jet technology very flexible in a hybrid-packaging environment where different component sizes and various packaging technologies are placed and/or underfill simultaneously.

Jetting Abrasive Underfill Materials

It has for some time a challenge to be able to jet abrasive materials consistently for extended periods of time due to the fact that the materials in contact with the abrasive fluid develop wearout that eventually affect the outcome of the jetted material. Although, this is indeed a fact with the

present materials used, the relevant issue is that of the time –to-affect the jetted material characteristics including geometry, volume and mass. Hence, one needs to understand the evolution of such wearout mechanism as function of actual operation and then determine its field mean life. Figure 12 depicts needle wearout evolution resulting from jetting abrasive underfill material, Dexter 4549.

Figure 11. Needle head wearout from jetting abrasive underfill material.

One can observe the increase on the area of that contour where the needle meets the seat of the jet by displacing the abrasive fluid present prior to impact.

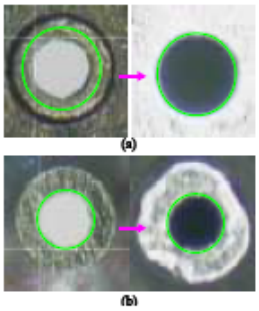

Figure 13. Nozzle wearout progress resulted from jetting abrasive materials: (a) Interior end of nozzle diameter. (b) Nozzle outside orifice.

Similar wearout can be observed on the nozzle; there the inner diameter has increase and some changes on the geometry (radius of curvature increased) that eventually will affect the volume of material jetted. This nozzle diameter increase is perhaps the parameter that would affect the size volume and shape of the material jetted the most for a given configuration. Figure 13 depicts the orifice of a time zero nozzle and that of a nozzle that have seen about eight million activations (jetted dots) of an abrasive material. There we can observe an increase on the orifice diameter of about 6% and the interior inside diameter increase of more than 40%. The variation in dot mass as function of time during the jet life test can be depicted in figure 14. Although some increase in mass is observed early, such trend ceased for a long time (35 million actuations to date).

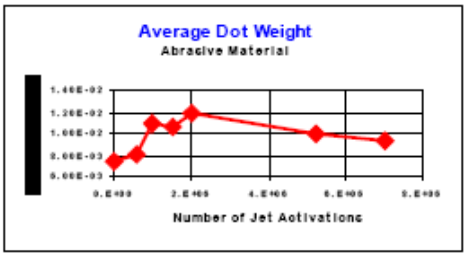

Figure 14. Dot mass average as function of jet activations.

It is expected that eventually if the orifice of the needle increases, the dot diameter will increase as well. Leakage of fluid near the seals is a potential problem from wearout of the needle caused by friction.

Findings

Throughout this study, several general trends were observed. It was found that the parameters that most consistently affected dot size were valve-on-time, seat size, temperature, and stroke length. A shorter valve on time seemed to correspond with smaller dots, perhaps because there is less time for material to flow beneath the ball-needle. With the jetting process, small dots were made at shorter valve-on-time. In addition to valve-on-time, the new design (smaller jet geometries) resulted in a significant improvement; dot diameter was reduced by 16 per cent without any impact on the dot quality. Because of the consistency of the underfill (it is similar to syrup or honey), perhaps greater force is needed to separate a drop from the rest of the fluid. Even with 4 turns of preload the stroke length may need to be longer to get the required compression of the spring in order to jet a dot. The final parameter affecting the size of the dots was the temperature the fluid was heated to. It was found that by adjusting the temperature and

leaving all other setting constant the dot size was not changed. However, when the fluid was heated to higher temperatures, the stroke length could be set lower before it began to clog. Therefore, with more heat, the stroke length could be set lower, giving smaller dots, so temperature indirectly affected dot size. The other adjustable parameters did not seem to influence dot size quite as much. Pressure was another parameter that had to be balanced. Pressure needed to be high enough to force fluid below and around the ball-needle when it was raised, but also not so high that the pressure to back pressure difference was too large. With a pressure much greater than the backpressure, a greater amount of fluid was jetted with each drop. However, even when varying pressure between 10 and 50 psi, the influence of this effect on dot size was small compared to the influence of other parameters. A final observation regarding the variability of dot size based on parameter settings is the potential benefit. The ability to adjust a few parameters and get dots which range in size from 12 mils diameter to greater than 30 mil in diameter, along with the ability to fire multiple dots in the same place (to get larger dots) makes the jetting technology an extremely versatile process.

Conclusions

Numerical analysis shows the analytical process for the jetting process and the role of various parameters on the fluid being jetted. There are geometric, thermal and mechanical parameters that can be manipulated to achieve various size dots. The mechanical and thermal parameters allow adjustments to dot size on a micro scale. Macro adjustments are made through geometric scaling of the ball-needle seat and the nozzle size. The ball-needle jet geometry is the most critical component for macro adjustments. The mechanical and temperature adjustments allow dot size tuning and definition of a print window for stable dot generation. Clearly there is a path for future geometries that will provide even smaller dots in the future. One of the alterations to the jet design that had the largest impact on the dot size was the switch from 20 to 15 mils seat. It is proposed here that a further reduction of the seat diameter may result in yet smaller dot diameters. From analytical work there are some indications that an increase of the nozzle length may also reduce dot size by the fact that backpressure is increased. By the ability of jetting underfill materials in small amounts, less than 0.01mg dots, it is now possible to underfill small die components under a non-contact system, with great consistency. Jetting of abrasive materials does cause wearout in some of the components of the jet, but consistency of jetted material both quality and quantity wise, is not affected significantly. In fact, small tuning of some of the jetting parameters may result in no change of the material dispensed. Above findings open the application field of the jet to cover a much larger variety of materials.

Acknowledgement

The authors would like to thank Mr. A.P. Babiarz for the experimental work and data analysis and to Mr. J. Vint for assistance with hardware issues during this study.

Reference

[1] A.F. Piracci, "SMA Dispensing Trends," Surface mount Technology, Jan 2001 ASR-0102117 Rev. A

[2] J. W. Daily and D.R.F. Harleman " Fluid Dynamics," Addison-Wesley, 1966, pp. 97-115.

[3] C. Lanczos, "The Variational Principles of Mechanic", University of Toronto Press, 1970, pp.359-369